Solar Energy 163 (2018) 526–536

Contents lists available at ScienceDirect

Solar Energy

journal homepage: www.elsevier.com/locate/solener

Irradiance intensity dependence of the lumped parameters of the three-diodes model for organic solar cells

Antonino Laudani[a,*], Francesco Riganti Fulginei[a], Fernando De Castro[b], Alessandro Salvini[a]

[a] Department of Engineering, Roma Tre University, V. Vito Volterra, 62, Roma I-00146, Italy
[b] National Physical Laboratory, Hampton Rd, Teddington, UK

ARTICLE INFO

Keywords:
Organic solar cells
PV modeling
I-V curve
Circuital model

ABSTRACT

In this paper the current-voltage characteristics of organic solar cells (OSC) is analyzed in terms of equivalent lumped parameter circuit at different level of insolation. In particular, starting from a circuital model based on a three-diode configuration, a set of formulas is proposed to describe the dependence of lumped circuital parameters on irradiance intensity and consequently the behaviour of organic solar cells from dark to high irradiance conditions. These expressions are achieved by using a trail and error approach applied to the fitting procedure of measured I-V curves at different irradiance levels. The achieved model with parameters dependent on irradiance level allows us to use a single circuit for the analysis of OSC under different operating conditions: this is the first step for the integration of OSC circuital model in photovoltaic system simulator, but also can furnish a novel point of view for the advance of the OSC applied research. Experimental measurements are used to setup the model and for its successive validation on two different kind of organic solar cells.

1. Introduction

The development of an equivalent circuital model for Organic Solar Cells (OSC) has been subject of study since the first solar cells appear in various laboratories. This is due to a twofold need: on the one hand these models are important to compare the behaviour of OSC with Silicon based one; on the other hand they can be useful for the development of effective energy production systems based on OSC only or their integration with traditional photovoltaic plants. Moreover, the classic circuital models, widely used for Si-based solar cells, cannot be used directly, since the most recently developed OSC, based on perovskite or other organic semiconductors (Reenen et al., 2015; Xu et al., 2016; Wagenpfahl et al., 2010) exhibit under illumination conditions some deformations of I-V characteristics that influence their energy conversion capability (Ortiz-Conde et al., 2012; Gaur and Kumar, 2014; Wagner et al., 2012; Saive et al., 2013; Zuo et al., 2014; Romero et al., 2014). That behaviour, also known as S-shape or kink effect, has been widely addressed in literature and different circuital solutions were proposed to face it (a wide review can be found in García-Sánchez et al. (2017)). Recently a three-diode circuit has been proposed able to model different OSC with a high accuracy, also in the case of an evident S-shape effect in $I-V$ curves (García-Sánchez et al., 2013; Castro et al., 2016; Roland et al., 2016). Clearly, other than the fitting of single $I-V$ curves for assigned irradiance and temperature values, the three-diode circuit is of interest also to verify if it is possible to derive a dependence on irradiance (and temperature) for the parameters of that equivalent circuit in order to describe, by a unique lumped parameter circuit, the cell behaviour in all the operating conditions (i.e. from dark one up to 200 mW/cm^2). Despite the fact that the behaviour in dark conditions appears in most cases really similar at a first sight to the traditional single diode model widely used for c-Si based devices, building a sole circuital model actually useful taking into account dark and irradiance conditions is not a trivial problem. Recently on this issue some good results have been achieved and presented in the work of Tada (2017) for some OSCs, by using a circuit containing only two diodes. Unfortunately the two-diode model is not able to describe current-voltage curve for devices exploiting high non linear S-shape as the one used in this work. Then, the aim of this paper is to find a new dependence of the parameters for the three-diode circuit by starting from the study of the identification problem at different irradiance values and from the use of a suitable simplified model under the dark condition. The herein proposed dependence of the lumped parameters of three diode configuration on irradiance level, allows us to use a single circuit for the analysis of OSC under different operating conditions: this is the first step for the integration of OSC circuital model in photovoltaic system simulator, but at the same time can furnish a novel point of view for the advance of the OSC applied research.

* Corresponding author.
E-mail addresses: alaudani@uniroma3.it (A. Laudani), riganti@uniroma3.it (F. Riganti Fulginei), fernando.castro@npl.co.uk (F. De Castro), asalvini@uniroma3.it (A. Salvini).

https://doi.org/10.1016/j.solener.2018.02.032
Received 9 September 2017; Received in revised form 13 January 2018; Accepted 12 February 2018
Available online 13 March 2018
0038-092X/

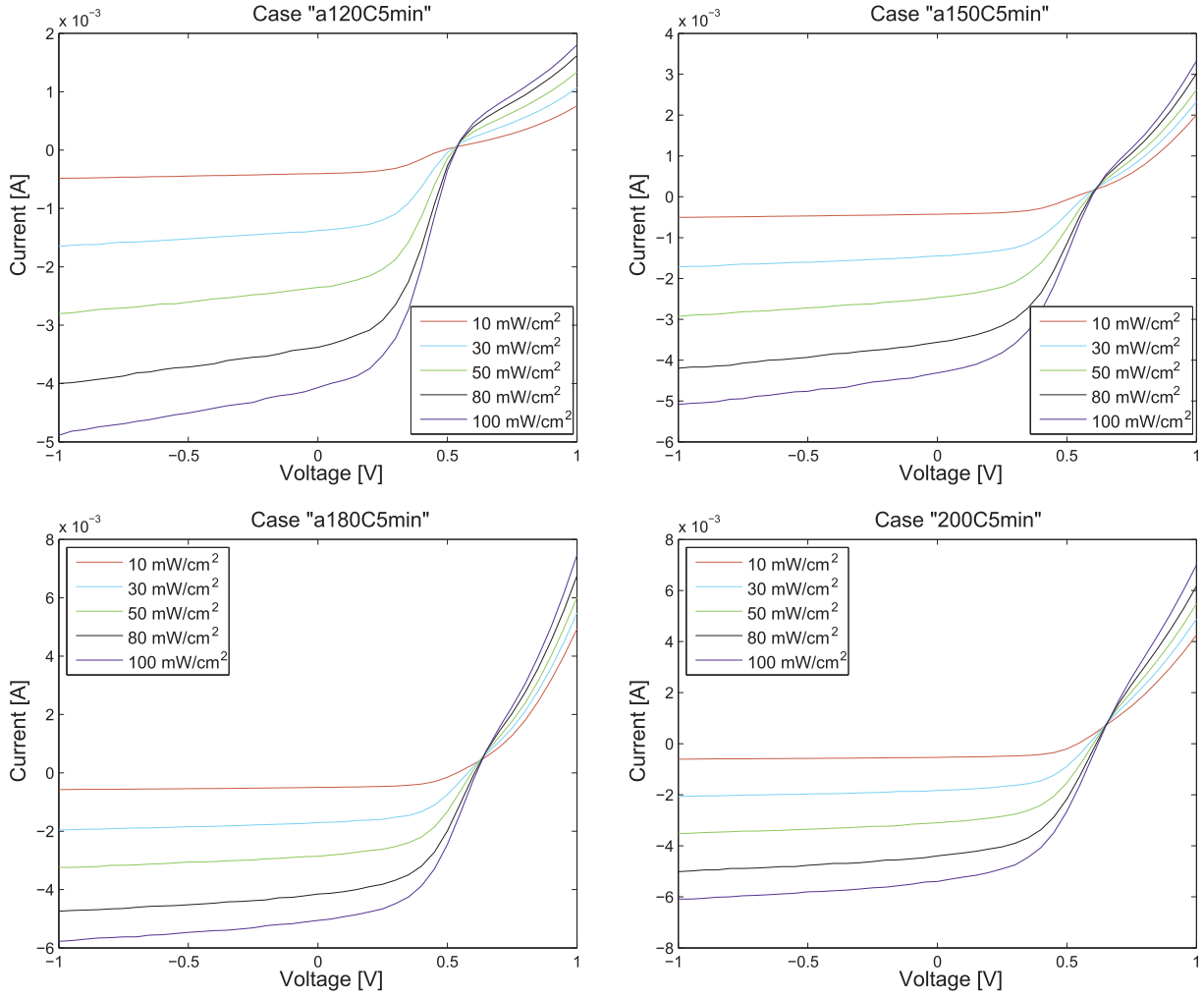

Fig. 1. Experimental OSC current-voltage curves at different insolation levels (from 10 mW/cm^2 to 100 mW/cm^2) for solar cells annealed at 120 °C, 150 °C, 180 °C, 200 °C for 5 min. It is worth noticing the non-ideal behaviour due to the strong S-shape effect.

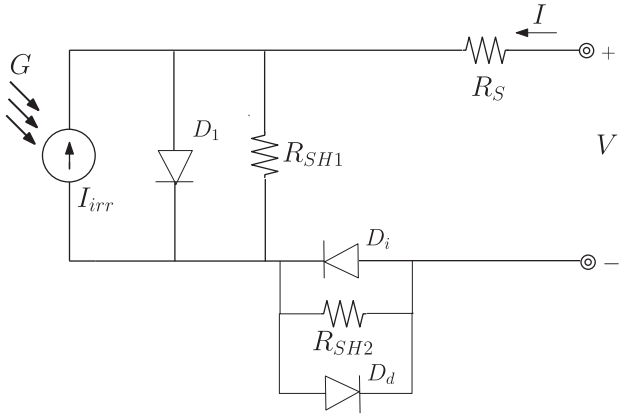

Fig. 2. Three-diode model for organic cells.

2. Measurements and experimental data

In our study we make use of solar cell devices consisting of an enhanced bi-layer of purified Poly[2-methoxy-5-(2-ethylhexyloxy)-1,4-phenylene-vinylene] (MEH-PPV, M_n = 40,000–70,000, Aldrich) acting as electron donor and fullerene C60 (>99.95%, SES Research) acting as electron acceptor. Films were fabricated on cleaned ITO-coated glass coated with 50 nm of PEDOT:PSS (Aldrich, conductivity 1 S cm^{-1}) and subsequently coated with 50 nm of Al to serve as the cathode (Castro et al., 2006; de Castro et al., 2010). Sample fabrication and characterization was performed in inert N_2 atmosphere. Details of device sample preparation and characterization were reported previously (Castro et al., 2006; de Castro et al., 2010) and are out of the scope of this work. Thermal annealing at different temperatures was used to reduce the s-shape as previously described (de Castro et al., 2010). In this work we fitted curves of devices not annealed and annealed for 5 min at 120 °C, 150 °C, 180 °C and 200 °C. We refer to these samples as “not annealed “ and a120C5min, a150C5min, a180C5min and a200C5min, respectively. It is worth noticing the presence of strong s-shape effects that have a tendency to disappear at low irradiance levels. As it is evident from Fig. 1 the current-voltage characteristic of these OSC presents significant modifications in behaviour according to its preparation and regions of operation. Although in the range voltage range 0−V_{OC} in some cases these curves are very similar to those of Si-C devices, it is also evident the strong nonlinear behaviour close to V_{OC} (see for example the case 120C5min in Fig. 1). This effect is typical of OSC having S-shape, but for these devices is also evident that, for voltage higher than V_{OC}, the current does not rise with a constant slope but instead with a exponential dependence. For these regions the devices cannot be modelled by means of simple two opposed diode model as done successfully for other devices by Tada (2017). On the other hand the introduction of a third diode allows to overcome this problem and, at the same time, modifies at minimum the shape of current-voltage characteristic for voltage values lower than V_{OC}.

For these samples experimental current-voltage curves at different

Table 1
Solutions of the identification problem for 120C5min case at different insolation levels.

	10 mW/cm^2	30 mW/cm^2	50 mW/cm^2	80 mW/cm^2	100 mW/cm^2
R_{SH1} [kΩ]	12.167	3.736	2.254	1.586	1.288
R_{SH2} [kΩ]	2.8740	0.7502	0.4953	0.3941	0.3658
I_{01} [μA]	0.3788	1.5892	4.1903	7.4225	6.9938
I_{0i} [mA]	0.0259	0.1108	0.1873	0.2838	0.3693
n_1V_T [V]	7.0196E − 2	7.6225E − 2	8.3090E − 2	8.7242E − 2	8.4231E − 2
n_iV_T [V]	2.6969E − 2	3.2877E − 2	3.2293E − 2	3.4149E − 2	3.8060E − 2
I_{irr} [mA]	0.4099	1.4058	2.4038	3.4393	4.1719
I_{0d} [μA]	113.72	24.165	7.1576	3.1205	3.2032
n_dV_T [V]	0.2426	0.1598	0.1216	0.1014	0.1012

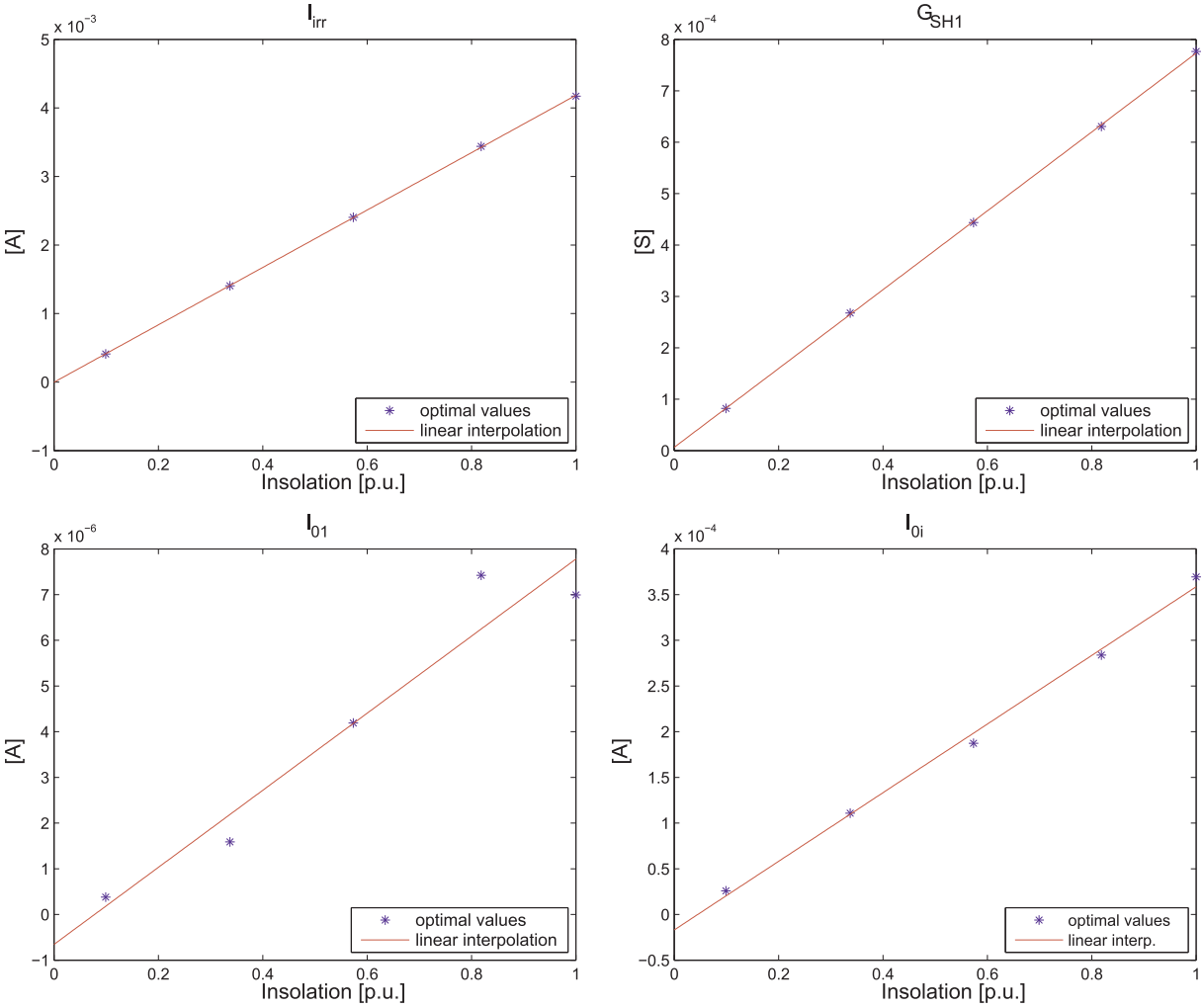

Fig. 3. I_{irr}, G_{SH1}, I_{01}, I_{0i} VS insolation.

level of irradiance from dark conditions to 100 mW/cm^2 simulated AM1.5G sunlight were measured under inert N_2 atmosphere. The experimental $I-V$ curves for these data are shown in Fig. 1, except for dark conditions which are shown separately in a next figure.

3. The one-equation model for the three-diode circuital representation of an OSC and its identification under light condition

The complete three-diode circuit under study is represented in Fig. 2. As it has been already demonstrated by Castro et al. (2016), for this circuit it is possible to achieve a single equation formula, useful for the solution of the identification problem. That formula is the following:

$$V_{Dd} = V - \left[(I + I_{irr} + I_{01})R_{SH1} - n_1 V_T W\left(\frac{I_{01}R_{SH1}}{n_1 V_T} e^{\frac{(I+I_{irr}+I_{01})R_{SH1}}{n_1 V_T}} \right) \right] - R_S I \quad (1)$$

$$V_{Di} = -V_{Dd} \quad (2)$$

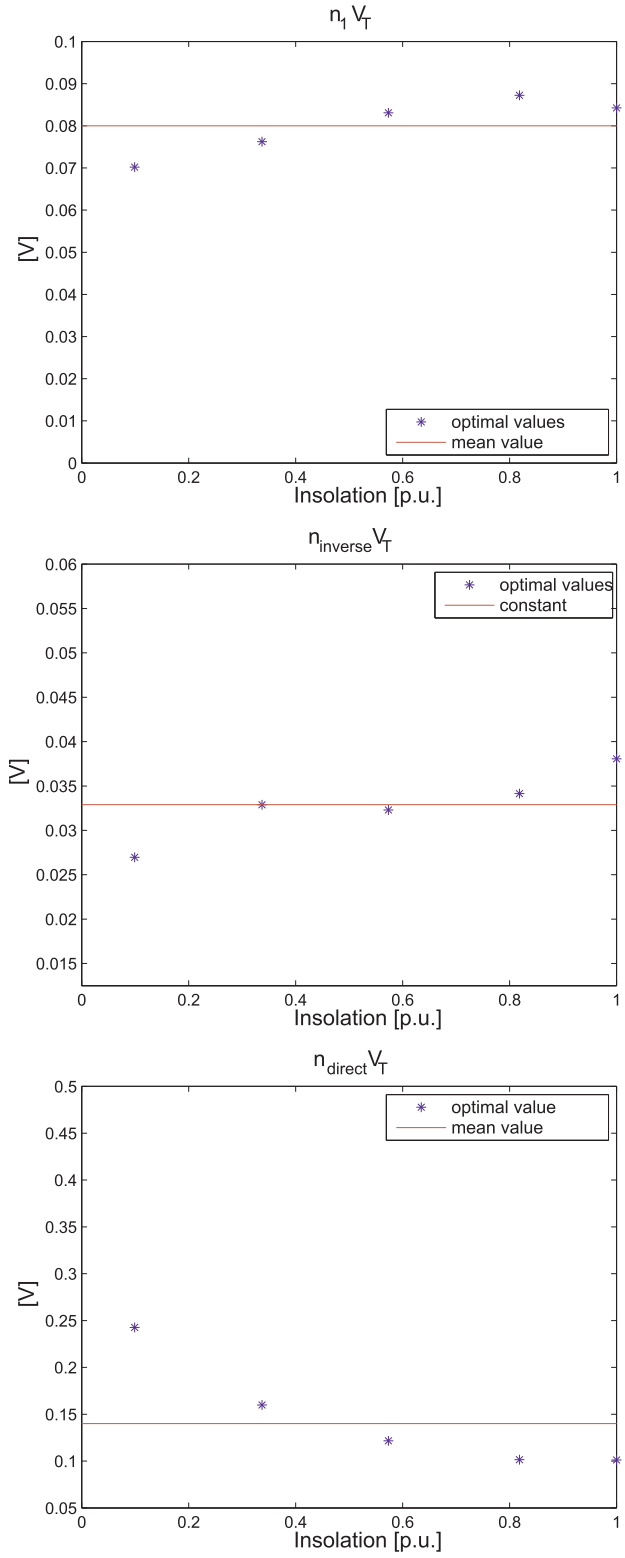

Fig. 4. Ideality factor of diodes D_1,D_i,D_d VS insolation.

$$I = \frac{V - \left[(I + I_{irr} + I_{01})R_{SH1} - n_1 V_T W\left(\frac{I_{01}R_{SH1}}{n_1 V_T} e^{\frac{(I+I_{irr}+I_{01})R_{SH1}}{n_1 V_T}}\right)\right] - R_S I}{R_{SH2}} - I_{0i}\left[e^{\frac{V - \left[(I+I_{irr}+I_{01})R_{SH1} - n_1 V_T W\left(\frac{I_{01}R_{SH1}}{n_1 V_T} e^{\frac{(I+I_{irr}+I_{01})R_{SH1}}{n_1 V_T}}\right)\right] - R_S I}{n_i V_T}} - 1\right] + I_{0d}\left[e^{\frac{V - \left[(I+I_{irr}+I_{01})R_{SH1} - n_1 V_T W\left(\frac{I_{01}R_{SH1}}{n_1 V_T} e^{\frac{(I+I_{irr}+I_{01})R_{SH1}}{n_1 V_T}}\right)\right] - R_S I}{n_d V_T}} - 1\right] \quad (3)$$

where V_{Di} and V_{Dd} are the direct voltages of the two diodes D_i and D_d respectively, V_T is the thermal voltage (equal to $\frac{k_B T}{q}$ where k_B is the Boltzmann constant, T is the temperature of the cell in Kelvin, and q is the elementary charge). The detailed algebraic manipulation of that formula can be found in Castro et al. (2016). In the Eq. (3), R_{SH1},R_{SH2},I_{01},I_{02},I_{03},n_1,n_2,n_3,I_{irr} and R_S are the 10 parameters to be determined according with a fitting procedure employing experimental data. As stated in Castro et al. (2016) in the solution of this identification problem it is possible to set $R_S = 0$ since it has been observed that this choice does not influence the behaviour of the three-diode circuit in the fitting of experimental results. Indeed it was observed by Castro et al. (2016) the problem of identification without this choice appears to be ill-posed, since multiple solutions with different values of R_S and similar values for the other parameters can be found. We remand the reader to the work of Castro et al. (2016) for a detailed discussion on this issue. From our point of view, this fact is very interesting also because allows to reduce the number of unknown parameters in the identification problem from ten to nine (Castro et al., 2016). The non-linear group consisting in D_i,D_d and R_{SH2} assumes the role of an equivalent non-linear series resistance. The possibility to exploit the one-equation formula (3) is really important since allows an easy implementation of the least squares error (LSE) procedure for fitting experimental data (see Castro et al., 2016 for further details).

3.1. Identification of the parameters at different irradiance conditions

All the available $I-V$ curves at different insolation levels, shown in Fig. 1, have been used to identify the nine parameters at different insolation levels. In the following we only present the results related to 120C5min case, but very similar results are achieved in all the examined cases. For the identification problem, we adopted a minimization approach using as objective function the Mean Squared Error (*MSE*), as already successfully done for inorganic solar cells/modules (Laudani et al., 2014a), defined as follows:

$$MSE = \frac{1}{N}\sum_{k=1}^{N} [I_k^{measured}(V_k^{measured}) - I_k^{computed}(V_k^{measured})]^2 \quad (4)$$

where N is the number of measurements $(I_k^{measured}, V_k^{measured})$ available, whereas $I_k^{computed}(V_k^{measured})$ is achieved by exploiting the Eq. (3). This objective function is utilized into a hybrid optimizer which combines stochastic and deterministic methods. In particular, we exploits the exploration capability of the Genetic Algorithm (GA) to individuate candidate solutions, and the strong convergence of the deterministic methods (such as Levemberg-Marquadt) implemented in the *fsolve* Matlab function. Thus, GA has been used for improving the exploration and *fsolve* has been introduced for the refinement of GA's solutions. In addition, we run 10 times the hybrid optimizer in order to get a better evaluation of results and to avoid falling into local minima that do not correspond with optimal solution for the parameters. Indeed, in this

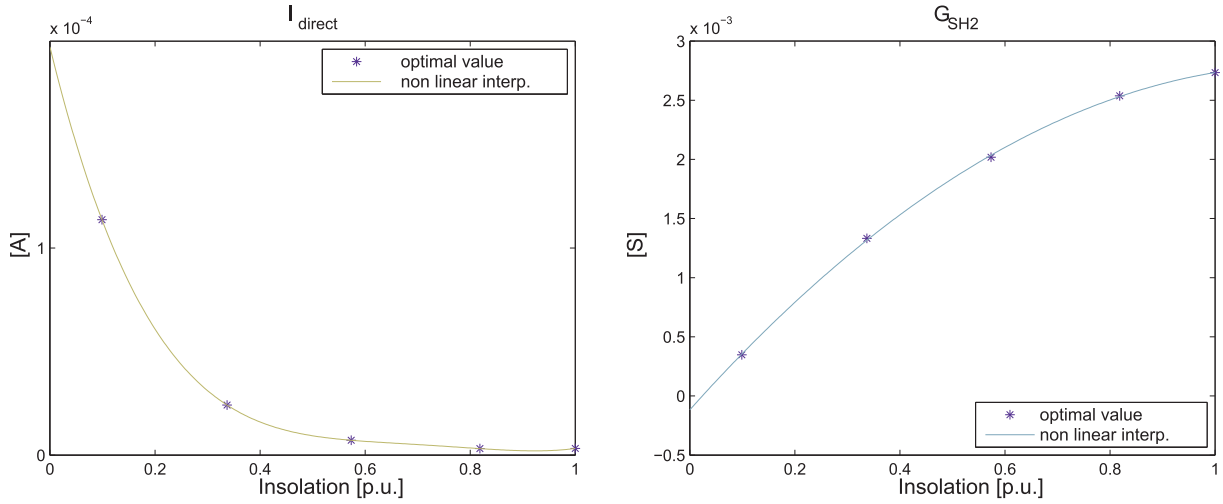

Fig. 5. Saturation current of diode D_d and G_{SH2} VS insolation.

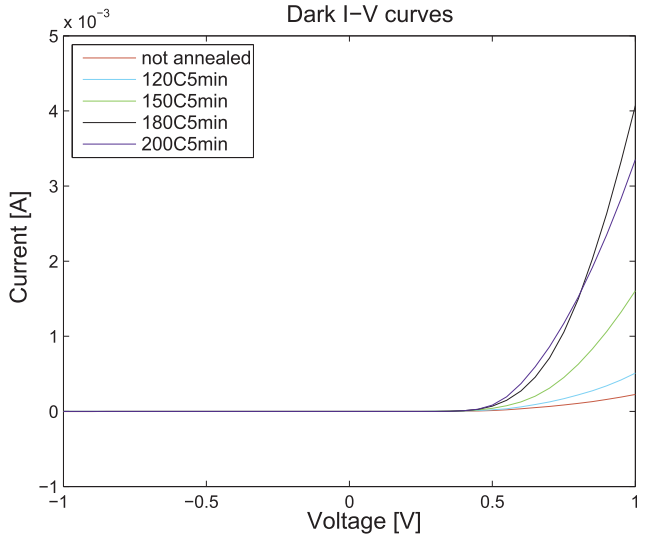

Fig. 6. Dark I-V curves used for tests.

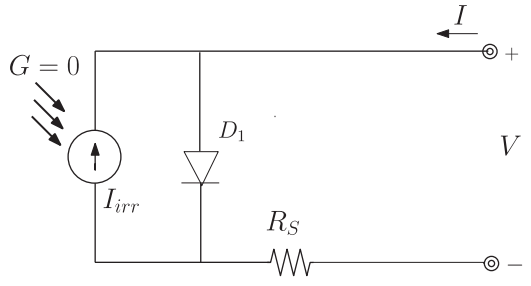

Fig. 7. One diode circuit without shunt resistance R_{SH}.

Table 2
Comparison among solutions obtained by the one diode model for dark condition with and without current source I_{irr}.

Parameter	With I_{irr}	Without I_{irr}
I_0 [μA]	2.1020E−01	1.9685E−01
nV_T [V]	0.10229	0.10127
R_S [Ω]	406.94	409.78
I_{irr} [A]	5.07754E−07	0
MSE	7.31E−12	7.48E−12

way we minimize the influence of initial guess used for the optimization/identification problem. A solution to the problem can be considered appropriate respect to the other candidate solutions when several launches lead to the same results and the MSE is lower than those of other candidate solutions. In our tests, usually most of the 10 attempts converge to the same results with lowest MSE and then the identificated parameters can be considered as appropriate. In Table 1 we report the results for all the insolation levels. It is worth noticing that in the identification problem, we work with the reciprocal of shunt resistances in such a way to manage all numbers lower than 1.0. For this reason the results are expressed either in terms of resistance or in terms of conductance.

The plots of the various parameters versus the insolation levels are shown in Fig. 3.

Remarks

From the identification of the parameters for $I-V$ curves at different insolation levels and the related plots shown in Figs. 3–5 it is possible to observe:

- I_{irr} linearly increases with insolation (as expected);
- G_{SH1}, I_{01} and I_{0i} show a similar dependence;
- All the ideality factors are almost constant;
- G_{SH2} increases with insolation more slowly than a linear behaviour;
- $I_{02direct} = I_{0d}$ drastically decreases with insolation;
- It is worth noticing that if the insolation $\longrightarrow$0 (dark condition), some of the parameters might reach the zero value. This means they might be removed from the circuit for the dark condition (see next paragraph).

These remarks are the starting point for the development of a model able to describe the behaviour of circuital parameters as functions of irradiance level. Clearly no physical explanation is done in the following study but just a “mathematical modelling” able to predict the results in the most accurate way possible. However in order to gain further insight into this issue, we provide a detailed analysis of the fitting problem by starting from the circuital model in dark conditions, as explained in the next section.

4. Circuital model for dark conditions

In this section we present the results achieved in the construction of a circuital model able to represent dark conditions. In order to do that, also considering the typical profile of $I-V$ in dark conditions (see for example Fig. 6), we start with the traditional one-diode model and add or remove circuital elements according to the decreasing of MSE

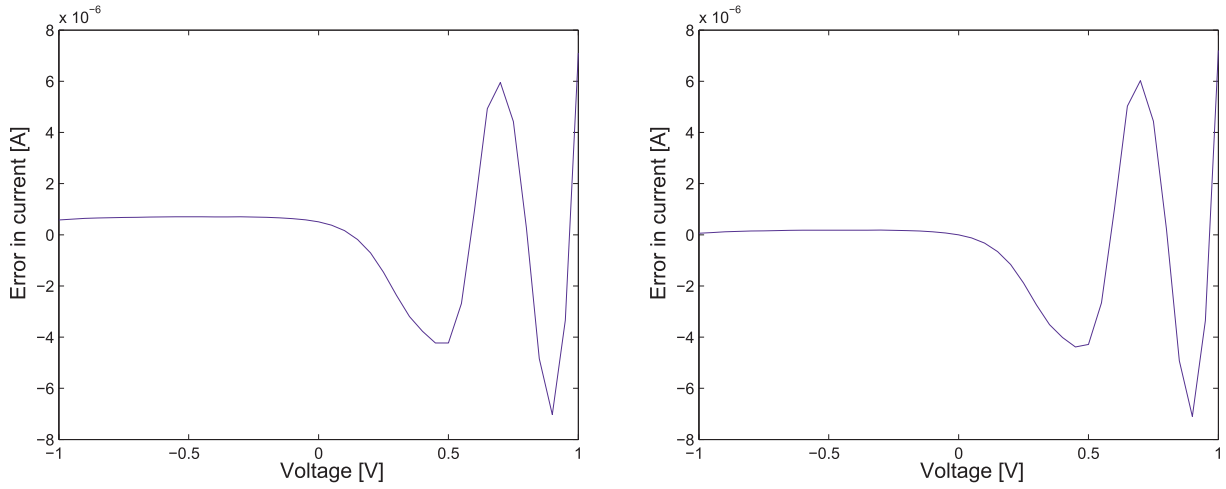

Fig. 8. Error in the fitting of one diode model with (left) and without (right) I_{irr}.

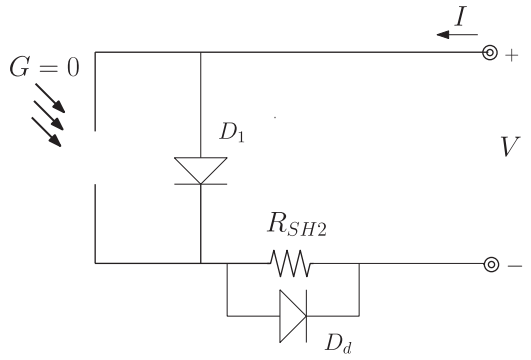

Fig. 9. Double diode circuit without shunt resistance R_{SH2}. The R_S is no longer present and R_{SH1} is again ∞.

Table 3
Solution obtained by the double diode model for dark condition (without I_{irr}).

Parameter	
I_{01} [μA]	9.043718E−03
n_1V_T [V]	0.062505779
I_{0d} [μA]	1.443720E+01
n_dV_T [V]	0.121351401
R_{SH2} [Ω]	963.65
MSE	1.051E−13

between computed and measured data. In our tests we have found very similar results for all the 5 cases available (shown in Fig. 6) but, for sake of simplicity, we only present the results achieved for the case 120C5min.

As stated before we start the analysis trying to use the traditional single diode model, widely adopted for modeling inorganic photovoltaic (Laudani et al., 2014b; Luque and Hegedus, 2011; Desoto et al., 2006). The five circuital elements describing this model are: an ideal current source I_{irr} ideally linked to irradiance level (also called photocurrent); a diode in anti-parallel to the current source and characterized by saturation current I_0 and ideality factor n; a resistance in parallel to current source, called shunt resistance R_{SH} and a series resistance R_S. The first achieved result was the necessity to set the value of R_{SH} to ∞ (the same is the $G_{SH} = 0$) in order to make effective the fitting procedure. Indeed the fitting procedure did not converge to "meaning" results without this hypothesis, i.e. it returns very rough results in terms of MSE even after several launches of the optimizer. Consequently the final considered circuit for dark condition is represented in Fig. 7. It is worth noticing that in our first test, the I_{irr} was assumed not null: indeed, even if theoretically a zero value should be taken into account, during the measurements not always the perfect dark condition are guarantee. However, in a successive test the I_{irr} was fixed to zero and we found the difference in terms of *MSE* and other parameter values between the case with $I_{irr} \neq 0$ and $I_{irr} = 0$ was practically negligible. Consequently we can assume that the dark condition is fully satisfied during our measurements also considering I_{irr} equal to zero. The parameters achieved in both cases are reported in Table 2, and the error in the fitting of one-diode model with and without I_{irr} is plotted in Fig. 8. As stated before the difference is practically negligible.

From the achieved numerical values, further considerations can be done, above all regarding R_S. Indeed, although with the model above the R_S should be viewed as a serie resistance linked to the contact loss, its very high value suggests that this cannot be the role/origin of this component. A better interpretation for this component can be that it is a part of a non-linear group constituted by a shunt resistance in parallel with another component that does not appear in the one-diode model: according to the model proposed in literature by Castro et al. (2016) this component should be a diode. This is also in accordance with the profile of the error that has an high irregular behaviour just for higher values of voltage. This second diode should act so as to short-circuit (bypass) the serie resistance R_S for high voltage and consequently it has the same direction of first diode. As a consequence of this remark, the second investigated circuit is the one presented in Fig. 9.

In the following the resistance previously named R_S has been renamed R_{SH2} and R_{SH1} value is again ∞. There are now 5 parameters to be identified: the saturation currents for both diodes, I_{01} and I_{0d}; the ideality factors (multiplied for thermal voltage $V_T = k_BT/q$) for both diodes n_1V_T and n_dV_T; and the shunt resistance R_{SH2}. The same previously adopted procedure was used and the results of this identification are reported in Table 3 and in Fig. 10.

By using this new circuit the performance of fitting has been improved: the *MSE* is now 1.05E−13, that is about 70 times lower. The improvement is really remarkable and also the maximum error is now lower than 1 μA, whereas previously it was about 7 μA. At this point the next step was to add a further element in parallel to the R_{SH2} (in no dark conditions this is made to take into account the kink behaviour Castro et al., 2016), see Fig. 11.

At this point, with another diode, we have two further parameters to be found: the saturation current, I_{0i}, and the ideality factor, n_iV_T, of the diode D_i (the pedix "i" denotes the inverse polarization of this diode with respect to the other two). The solution of the identification problem by using the same previously described approach, leads us to the following considerations: the performance in terms of MSE improves

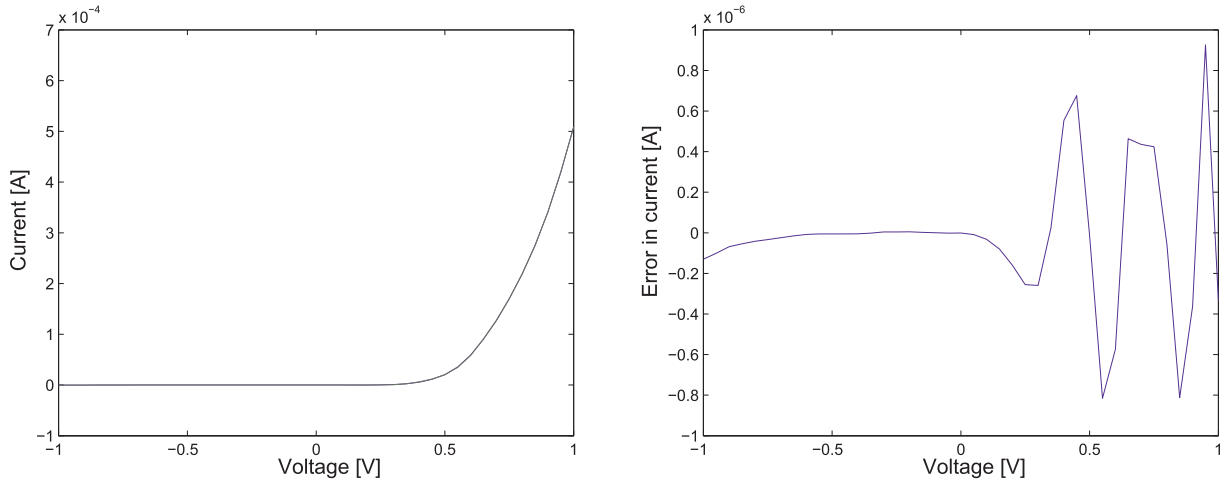

Fig. 10. Comparison between measured and double diode I-V simulated curve and respective difference.

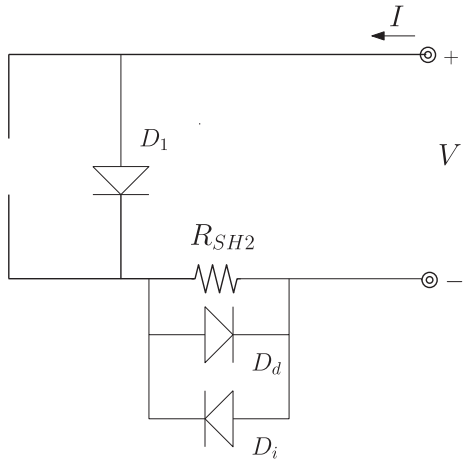

Fig. 11. Three-diodes circuit without shunt resistance R_{SH1}.

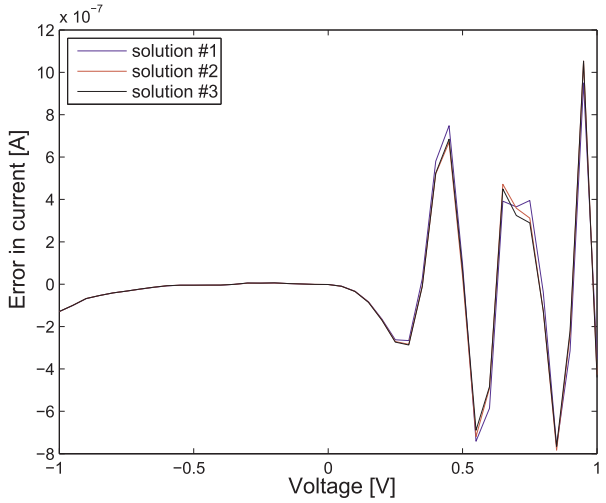

Fig. 12. Error for the three solutions presented in Table 4 for Three-diodes circuit.

Table 4
Three solutions obtained for the triple-diode model for dark condition.

Parameter	Sol # 1	Sol #2	Sol # 3
I_{01} [μA]	9.6142E−03	9.8156E−03	9.9766E−03
n_1V_T [V]	0.063232	0.063278	0.063460
I_{0i} [μA]	3.556298	5.2887E+01	1.3835E+01
n_iV_T [V]	0.030024	0.354780	0.135476
I_{0d} [μA]	1.5055E+01	1.5570E+01	1.5572E+01
n_dV_T [V]	0.121370	0.121421	0.121431
R_{SH2} [Ω]	964.31	1082.92	1009.21
MSE	1.016E−13	1.008E−13	9.838E−14

slightly (9.83E−14 with respect to 1.051E−13) but, at the same time, some problems in the identification arise. Indeed, multiple solutions with very similar MSE were achieved, with a remarkable difference above all in the parameters of diode D_i, I_{0i} and n_iV_T (three solutions are reported in Table 4) (see Fig. 12).

In our opinion, this is due to the fact that the identification problem is ill-posed if the third diode is taken into account in dark conditions, as if the number of parameters becomes too much large. On the other hand, we know that: (i) the diode D_i is important, since it allows us to model the kink effect as explained in de Castro et al. (2010); (ii) the presence of the diode D_d allows us also to justify the exponential increasing of the current modulus after the open circuit voltage; (iii) any attempt to remove R_{SH2} from the above circuit makes the identification

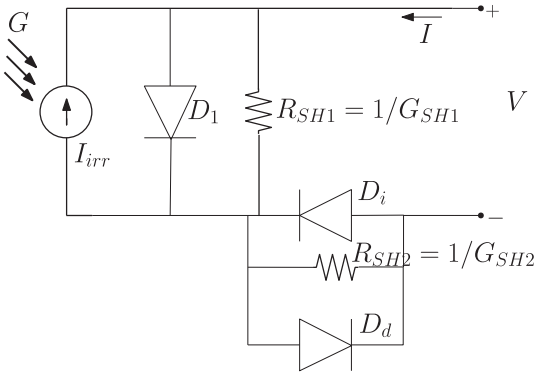

Fig. 13. Three-diode circuit valid for dark and irradiance conditions. The lumped elements are 6, but 12 parameters are used to model their dependence on irradiance level.

problem almost unsolvable, since the fitting procedure does not converge to solutions with acceptable *MSE*. Thus, with the aim to justify the presence of diode D_i, we assume the dependence of the saturation current of the diode D_i on irradiance level and in particular we assume $I_{0i} = 0$ in dark conditions. This allow us to maintain in operation the diode D_i when light affects the cell, where it seems to have an actual role. In this way the circuit in Fig. 11 matches with the one in Fig. 9 in dark conditions since $I_{0i} = 0$. Further details will be done in the next section where a model comprehensive of all the dependence of

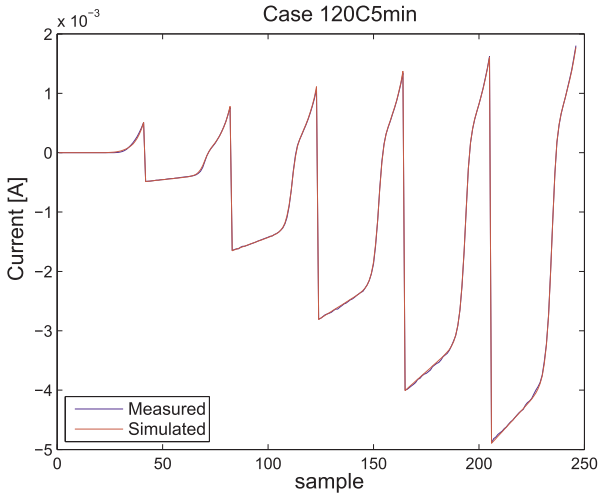

Fig. 14. Comparison between measured and simulated I-V curves for different levels of insolation for case 120C5min.

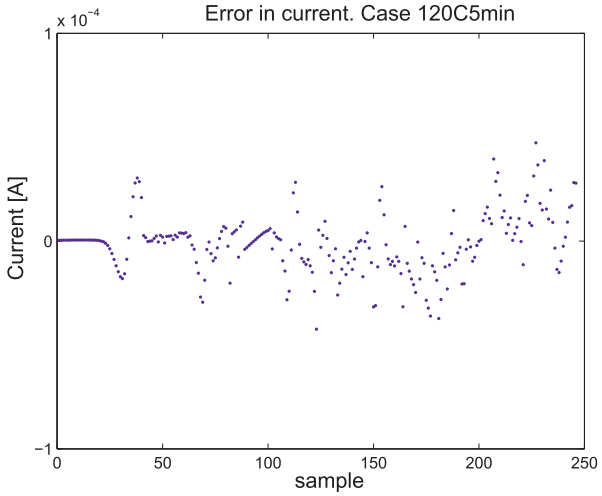

Fig. 15. Error between measured and simulated I-V curves for different levels of insolation for case 120C5min (***MSE = 2.0566E-10***).

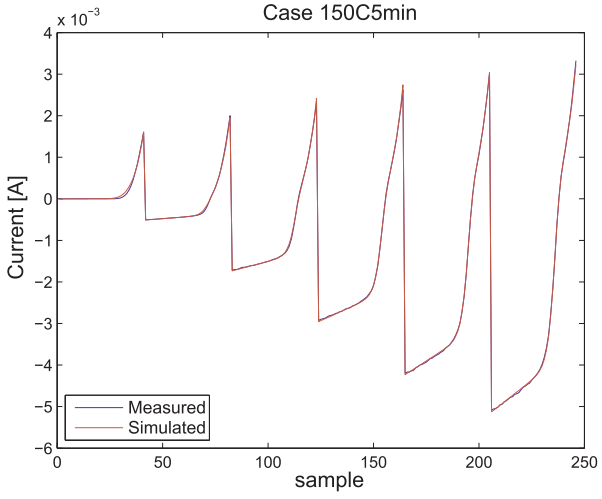

Fig. 16. Comparison between measured and simulated I-V curves for different irradiance levels for case 150C5min.

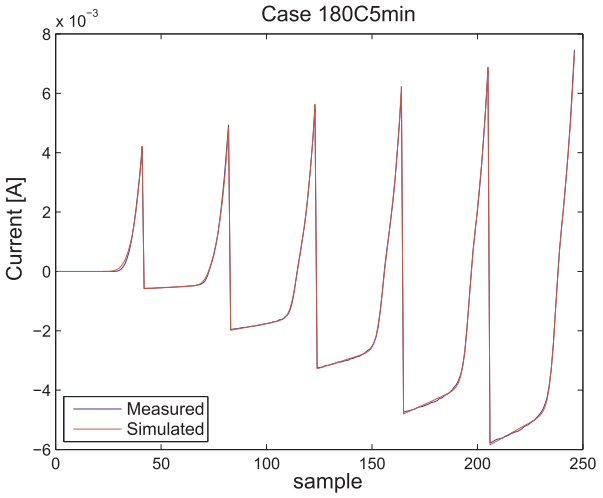

Fig. 17. Comparison between measured and simulated I-V curves for different irradiance levels for case 180C5min.

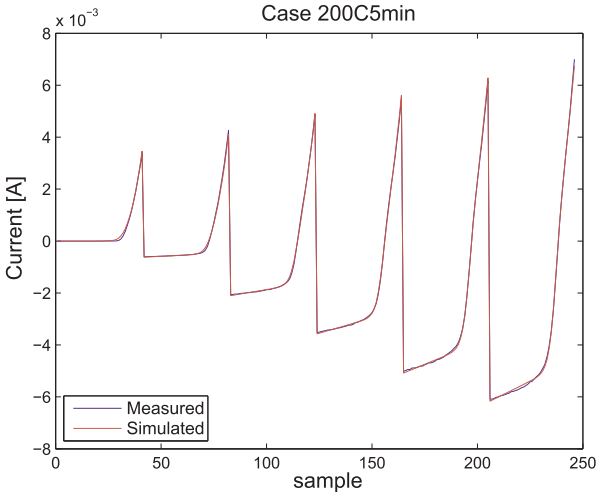

Fig. 18. Comparison between measured and simulated I-V curves for different irradiance levels for case 200C5min.

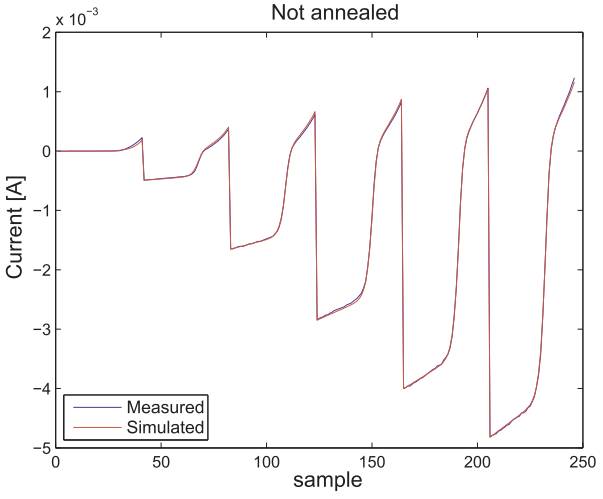

Fig. 19. Comparison between measured and simulated I-V curves for different irradiance levels for case “not annealed”.

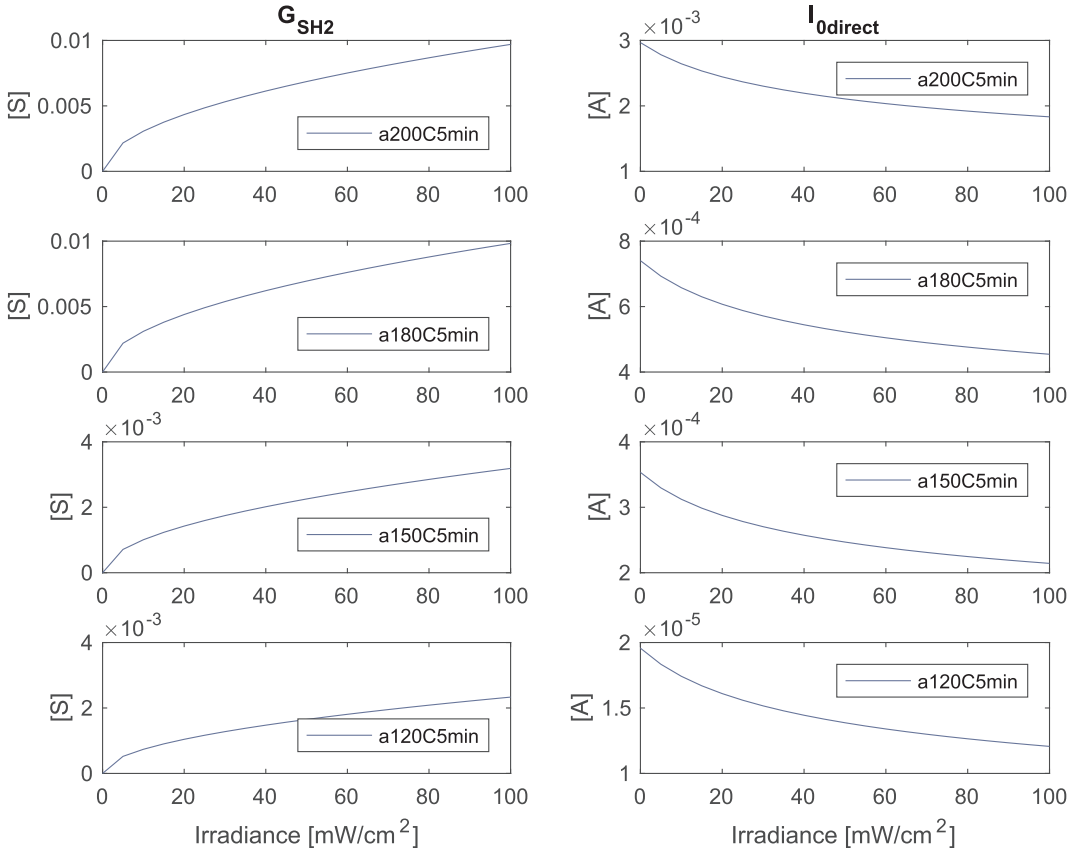

Fig. 20. G_{SH2} and $I_{0direct}$ vs irradiance level for the different annealed cases.

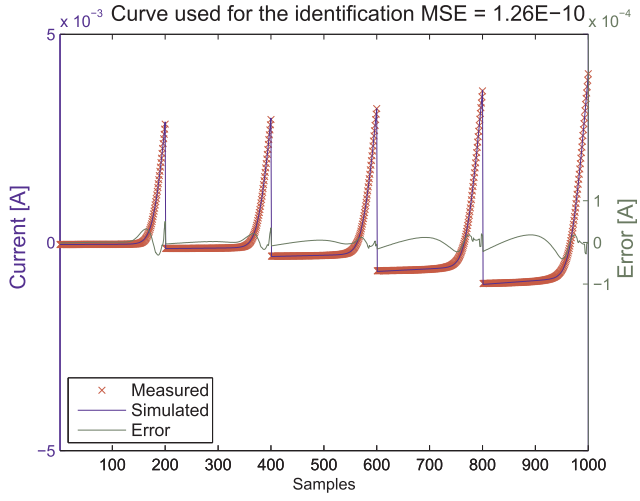

Fig. 21. Comparison between experimental and simulated curve and respective error for the samples used for the identification of the three diode models parameters for PTB7 cell.

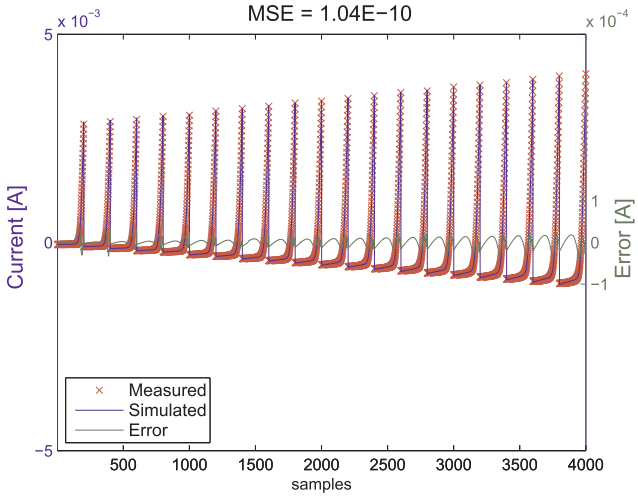

Fig. 22. Comparison between experimental and simulated curve for all the curves at different insolation available for PTB7 cell.

parameters on irradiance levels is presented.

5. A proposal for the irradiance dependence of parameters under insolation condition: set up and validation

In order to develop a model valid for describing the dependence on insolation conditions we proceed by using only the dataset named “120C5min”, that one might call “training” dataset just to indicate that it was adopted to study the dependence by means of a trial and error procedure, in order to empirically find some kind of possible dependence, considering all the available measurements. Validations are made by using the remaining four dataset (150C5min, 180C5min, 200C5min and “not annealed”). Then it was further used for another measured dataset named PTB7 in order to verify if the proposed formulas for irradiance dependence can be considered valid also for a more general case involving a Plastic PTB7 based solar cell.

From tests performed on 120C5min data, we propose the 12-parameter model represented by circuit in Fig. 13 together with the equations, empirically obtained, that define the dependence with respect to insolation S by means of “$S_{norm} = S/(100\ \mathrm{mW/cm^2})$” (the 12 parameters are in “bold” within the equations).

$$I_{irr}(S_{norm}) = S_{norm}\,\mathbf{I_{irr,norm}} \tag{5}$$

$$G_{SH1}(S_{norm}) = S_{norm}\mathbf{G_{SH1,norm}} \quad (6)$$

$$I_{01}(S_{norm}) = S_{norm}(\mathbf{I_{01,norm}} - \mathbf{I_{01,dark}}) + \mathbf{I_{01,dark}} \quad (7)$$

$$n_1 V_T(S_{norm}) = \mathbf{n_{1,norm}}\mathbf{V_T} \quad (8)$$

$$G_{SH2}(S_{norm}) = \sqrt{S_{norm}}(\mathbf{G_{SH2,norm}} - \mathbf{G_{SH2,dark}}) + \mathbf{G_{SH2,dark}} \quad (9)$$

$$I_{0i}(S_{norm}) = S_{norm}\mathbf{I_{0i,norm}} \quad (10)$$

$$n_2 V_T(S_{norm}) = \mathbf{n_{i,norm}}\mathbf{V_T} \quad (11)$$

$$I_{0d}(S_{norm}) = \frac{\mathbf{I_{0d,*}}}{\sqrt[\alpha]{S_{norm}} + \mathbf{S_{corr}}} \quad (12)$$

$$n_3 V_T(S_{norm}) = \mathbf{n_{d,norm}}\mathbf{V_T} \quad (13)$$

where $\mathbf{S_{corr}}$ is a dimensionless number introduced to consider the correction at dark condition, and α was set to 4. The choice of this value for α is due to a trial and error approach starting from interpolation of data shown in Fig. 5.

It is worth noticing that $\mathbf{I_{irr,norm}}$,$\mathbf{G_{SH1,norm}}$,$\mathbf{G_{SH2,norm}}$,$\mathbf{n_{1,norm}}\mathbf{V_T}$,$\mathbf{I_{01,norm}}$,$\mathbf{I_{0i,norm}}$,$\mathbf{n_{i,norm}}\mathbf{V_T}$ and $\mathbf{n_{d,norm}}\mathbf{V_T}$ are the parameters referred to an irradiance level of 100 mW/cm^2, while $\mathbf{I_{01,dark}}$,$\mathbf{G_{SH2,dark}}$ are the parameters referred to the dark condition. Clearly, in order to have physical meaning in any irradiance conditions, the parameters of Eqs. 7 and 9 must be bounded: in particular $\mathbf{I_{01,dark}} \geqslant 0$ and $\mathbf{I_{01,norm}} \geqslant \mathbf{I_{01,dark}}$ since the $\mathbf{I_{01}}$ increases with irradiance; similarly $\mathbf{G_{SH2,norm}} \geqslant \mathbf{G_{SH2,dark}}$ and $\mathbf{G_{SH2,dark}} \geqslant \mathbf{0}$. The results for this "training" case 120C5min are shown in Figs. 14 and 15 where we reported in succession all the $I-V$ curves available from dark to higher insolation level. The identification of the parameters was made considering all the available $I-V$ curves (six $I-V$ curves from dark to 100 mW/cm^2 of irradiance, composed by 40 samples each one) and solving the least squares problem by using the formulas (5)–(13) to take into account the different level of insolation and assuming that the temperature was constant and equal to 25 °C. The convergence was very fast due to the use, as initial guess, of the solution obtained from the previous simulation at 100 mW/cm^2. On the other hand, the computational cost can be considered acceptable even if these initial guesses data are not available: indeed, the repeating the identification process starting from different initial guesses, as explained before for the concept of the appropriateness of solution, leads to the same or similar results with lowest MSE in the 50% of cases examined in our tests. In terms of time for this fitting it is possible estimate that in a notebook with Intel i5 processor the elapsed time for ten runs is lower than half an hour. It is evident from these figures that the model "fits" the data very well and the proposed dependence on the irradiance level seems to work.

Obviously, you might think that the goodness of the obtained results could be due to a stroke of luck or limited to that dataset only. Nevertheless, the fitting results are extremely good also on all the other available data not used during the "training" step. Indeed the same model has been used for all the dataset available (150C5min, 180C5min, 200C5min, "not annealed") and the correspondent results are shown in Figs. 16–19.

The proposed formulas are quite simple since the three ideality factors are assumed indepenent of irradiance, other four parameters have linear dependence, whereas only G_{SH2} and I_{0d}, that is saturation current of direct diode, have a non linear dependence on irradiance. In Fig. 20 the results achieved in terms of behaviour vs irradiance level for the previous case are plotted for these two parameters.

The results achieved confirm the possibility to exploit this model at different levels of irradiance just considering the dependence expressed in the Eqs. (5)–(13): this might give the possibility to develop specific circuit for optimization of energy production in OSC based photovoltaic systems. As further validation another data-set is used in next section.

5.1. Test with Plastic PTB7 cell

The results presented in this section refer to another kind of organic solar cell, based on polymer PTB7 and consequently named herein PTB7 cell. The procedure followed for the identification of the parameters was a bit different since in this case we have 20 $I-V$ curves from 10 mW/cm^2 to 200 mW/cm^2 at step of 10 mW/cm^2 and each curve have 200 $I-V$ samples. For this reason we have chosen five $I-V$ curves to identify the parameters and then to use the parameters found to predict the behaviour for the other level of irradiance and comparing simulated results with measurements. As it is shown in the following, also in this case the model returns good results. In particular our choice was to use $I-V$ curves at 10 mW/cm^2,30 mW/cm^2,70 mW/cm^2,140 mW/cm^2 and 200 mW/cm^2 for the identification (this choice is however arbitrary since other tentatives have led to similar results). The results of fitting for this case is shown in Fig. 21, where the error between experimental and simulated curves is reported for all the 1000 samples used for the identification: *MSE* is very low and equal to $1.26E-10$. Fig. 22 shows the same plots for all the available data. Also in this case it is remarkable the very good matching between the simulated and experimental data for all the available data and the MSE, even lower than the one obtained in the previous case, demonstrates that the model works well in the whole range of available data.

6. Conclusions

In this paper a circuital model based on a three-diode configuration has been used to describe the behaviour of organic solar cells from dark to high irradiance conditions. An accurate analysis has been conducted starting from the classic one-diode model to the final three-diode model in which 12 parameters have to be found for the model identification at different irradiance levels. The parameters calculation is facilitated by a suitable mathematical approach, one-equation model, described within the paper. Moreover, a set of empirical equations has been introduced for describing the dependence of the lumped parameter model on irradiance level. The three-diode model, with parameters value dependent on irradiance level, allows us to use a single circuit for the analysis of OSC under different operating conditions: this is the first step for the integration of OSC circuital model in photovoltaic system simulator, but also can furnish a novel point of view for the advance of the OSC applied research. Very good results have been obtained by comparing experimental measurements with simulated I-V curves on different kind of organic solar cells.

References

de Castro, F., Heier, J., Nuesch, F., Hany, R., 2010. Origin of the kink in current-density versus voltage curves and efficiency enhancement of polymer-c60 heterojunction solar cells. IEEE J. Select. Top. Quant. Electron. 16, 1690–1699.
Castro, F.A., Benmansour, H., Graeff, C.F.O., Nüesch, F., Tutis, E., Hany, R., 2006. Nanostructured organic layers via polymer demixing for interface-enhanced photovoltaic cells. Chem. Mater. 18, 5504–5509.
Castro, F.D., Laudani, A., Fulginei, F.R., Salvini, A., 2016. An in-depth analysis of the modelling of organic solar cells using multiple-diode circuits. Solar Energy 135, 590–597.
Desoto, W., Klein, S., Beckman, W., 2006. Improvement and validation of a model for photovoltaic array performance. Solar Energy 80, 78–88.
García-Sánchez, F.J., Romero, B., Lugo-Muñoz, D.C., Pozo, G.D., Arredondo, B., Liou, J.J., Ortiz-Conde, A., 2017. Modelling solar cell S-shaped I-V characteristics with DC lumped-parameter equivalent circuits – a review. Facta Universitatis - Ser.: Electron. Energe. 30, 327–350.
García-Sánchez, F., Lugo-Muñoz, D., Muci, J., Ortiz-Conde, A., 2013. Lumped parameter modeling of organic solar cells S-shaped I-V characteristics. IEEE J. Photovolt. 3, 330–335.
Gaur, A., Kumar, P., 2014. An improved circuit model for polymer solar cells. Prog. Photovolt.: Res. Appl. 22, 937–948.
Laudani, A., Fulginei, F.R., Salvini, A., 2014a. High performing extraction procedure for the one-diode model of a photovoltaic panel from experimental I-V curves by using reduced forms. Solar Energy 103, 316–326.
Laudani, A., Fulginei, F.R., Salvini, A., 2014b. Identification of the one-diode model for photovoltaic modules from datasheet values. Solar Energy 108, 432–446.

Luque, A., Hegedus, S., 2011. Handbook of Photovoltaic Science and Engineering. John Wiley & Sons.
Ortiz-Conde, A., Lugo-Muñoz, D., Garcí-Sánchez, F.J., 2012. An explicit multiexponential model as an alternative to traditional solar cell models with series and shunt resistances. IEEE J. Photovolt. 2, 261–268.
van Reenen, S., Kemerink, M., Snaith, H.J., 2015. Modeling anomalous hysteresis in perovskite solar cells. J. Phys. Chem. Lett. 6, 3808–3814. PMID: 26722875.
Roland, P.J., Bhandari, K.P., Ellingson, R.J., 2016. Electronic circuit model for evaluating S-kink distorted current-voltage curves. In: 2016 IEEE 43rd Photovoltaic Specialists Conference (PVSC), pp. 3091–3094.
Romero, B., Pozo, G.D., Destouesse, E., Chambon, S., Arredondo, B., 2014. Circuital modelling of s-shape removal in the current voltage characteristic of tiox inverted organic solar cells through white-light soaking. Org. Electron. 15, 3546–3551.
Saive, R., Mueller, C., Schinke, J., Lovrincic, R., Kowalsky, W., 2013. Understanding S-shaped current-voltage characteristics of organic solar cells: Direct measurement of potential distributions by scanning kelvin probe. Appl. Phys. Lett. 103, 243303.
Tada, K., 2017. Validation of opposed two-diode equivalent-circuit model for S-shaped characteristic in polymer photocell by low-light characterization. Org. Electron. 40, 8–12.
Wagenpfahl, A., Rauh, D., Binder, M., Deibel, C., Dyakonov, V., 2010. S-shaped current-voltage characteristics of organic solar devices. Phys. Rev. B 82, 115306.
Wagner, J., Gruber, M., Wilke, A., Tanaka, Y., Topczak, K., Steindamm, A., Hörmann, U., Opitz, A., Nakayama, Y., Ishii, H., Pflaum, J., Koch, N., Brütting, W., 2012. Identification of different origins for S-shaped current voltage characteristics in planar heterojunction organic solar cells. J. Appl. Phys. 111, 054509.
Xu, F., Zhu, J., Cao, R., Ge, S., Wang, W., Xu, H., Xu, R., Wu, Y., Gao, M., Ma, Z., Hong, F., Jiang, Z., 2016. Elucidating the evolution of the current-voltage characteristics of planar organometal halide perovskite solar cells to an S-shape at low temperature. Solar Energy Mater. Solar Cells 157, 981–988.
Zuo, L., Yao, J., Li, H., Chen, H., 2014. Assessing the origin of the S-shaped I-V curve in organic solar cells: an improved equivalent circuit model. Solar Energy Mater. Solar Cells 122, 88–93.